



The effect of varying volume fraction of microcapsules on fresh, mechanical and self-healing properties of mortars



A. Kanellopoulos*, P. Giannaros, A. Al-Tabbaa

Department of Engineering, University of Cambridge, Trumpington Street, Cambridge CB2 1PZ, UK

HIGHLIGHTS

- Polymeric microcapsules with sodium silicate used for self-healing in mortars.
- Inclusion of microcapsules does not affect hydration and setting time.
- Increasing dosage of microcapsules slightly increases dramatically the viscosity.
- Increasing dosage of microcapsules slightly reduces the mechanical properties.
- Microcapsules showed good adhesion to the cement matrix.

ARTICLE INFO

Article history:

Received 16 February 2016

Received in revised form 20 June 2016

Accepted 22 June 2016

Keywords:

Self-healing
Microcapsules
Fresh properties
Mechanical properties
Fracture

ABSTRACT

Spherical polymeric microcapsules, carrying liquid sodium silicate, were used for autonomic self-healing of mortars. Microcapsules were added at varying volume fractions (V_f), with respect to the cement volume, from as low as 4% up to 32% and their effect on fresh, mechanical and self-healing properties was investigated. For this purpose a series of techniques were used ranging from static mechanical testing, ultrasonic measurements, capillary sorption tests and optical microscopy. A detailed investigation was also carried out at the microstructural level utilising scanning electron microscopy (SEM) and energy-dispersive X-ray spectroscopy (EDX). Results showed that although increasing V_f resulted in a $\sim 27\%$ reduction in the mechanical properties, the corresponding improvement in the self-healing potential was significantly higher. Areal crack mouth healing reached almost 100%. Also, the measured crack depth and sorptivity coefficient reduced to a maximum of 70% and 54% respectively in microcapsule-containing specimens. SEM/EDX observations showed that the regions in the periphery of fractured microcapsules are very dense. In this region, high healing product formation is also observed. Elemental analysis revealed that these products are mainly ettringite and calcium-silicate-hydrate (C-S-H).

© 2016 The Authors. Published by Elsevier Ltd. This is an open access article under the CC BY license (<http://creativecommons.org/licenses/by/4.0/>).

1. Introduction

Amongst the self-healing techniques developed in the last twenty years the microencapsulation approach is by far the most studied. Microencapsulation was initially developed for self-healing applications in polymers and composites [1] and developed from the previous systems based on hollow capillary tubes [2]. The two techniques have many similarities, but the use of microcapsules alleviates the manufacturing related issues associated with the incorporation of hollow tubes in matrices. Typically microcapsules have sizes ranging from few microns up to 1 mm, whereas hollow tubes have diameters and lengths ranging from 1 to 5 mm and 10–80 mm respectively. In principle, microcapsules

are containers that envelope a healing compound keeping it protected from the manufacturing processes as well as from the surrounding host matrix. The most fundamental principle of self-healing via microencapsulation is that the microcapsules are homogeneously dispersed in the bulk volume of the host material and the release of their healing compound is triggered by the formation of cracks that rupture their shell. Consequent chemical interactions between the encapsulated material(s) and the host matrix heal the crack. In this way, bulk material properties can be partially, or fully, restored.

There is a large number of different techniques and processes that produce an impressive spectrum of different types of microcapsules [3–5]. A wide variety of materials have been investigated as shell and core constituents in the microencapsulate systems. Polymeric shells and epoxy-based cargos are the most broadly used and investigated. The main focus of research over the last

* Corresponding author.

E-mail address: ak880@cam.ac.uk (A. Kanellopoulos).

fifteen years was on the actual development of these systems as well as the optimisation of the production techniques. This involved systematic investigation of the influence of the process parameters such as the agitation speed, the pH, the temperature and the concentration of raw materials on the size, stability, morphology, content loading and mechanical properties of the produced microcapsules [6–9]. In the last few years the concept of using microcapsules has extended to construction materials. While the microcapsules' production techniques do not differ significantly for such applications, the survivability, stability and functionality of microcapsules have been investigated for these non-polymeric host matrices [10–13].

Since the microcapsules are additions within the bulk volume of the host matrix it is expected they will alter its mechanical properties. The degree of this change depends on a large number of parameters: the size and the volume fraction of microcapsules, the mechanical properties of the shell materials and the mechanical interlock between the microcapsules and the surrounding matrix. The extent of self-healing itself depends on four major factors: the type of the healing compound used, the size of the crack, the size of the microcapsules and their volume fraction with respect to the bulk material. In cases where an activator is needed to promote healing, the quality, the particle size and the concentration of the activator also play an important role. It is therefore apparent that the ideal self-healing material should have an optimised balance between an alteration in its original properties due to the inclusion of microcapsules, and the potential self-healing efficiency.

Although a very large number of scientific articles discuss all the above mentioned parameters, the studies focusing on the effect of microcapsule addition on the mechanical properties of hardened cementitious matrices under static and dynamic load conditions are limited. Similarly, studies reporting on the effect of microencapsulate additions on the fresh properties, such as viscosity and curing time, are even scarcer. Brown et al. [14], in one of the most comprehensive studies on the effect of microcapsule addition on epoxy matrices-reporting that both the elastic modulus and ultimate stress decreased when increasing the percentage of microcapsules. More specifically they investigated microcapsule additions from as low as 6%, by volume of host matrix, up to 33%. The maximum reduction in elastic modulus and ultimate stress was reported as 30% and 64% respectively, for 33% of microcapsules, when compared to a matrix without additions. These findings verified similar trends reported earlier in the literature for epoxy composites containing polymeric microcapsules or microspheres [15–17]. Although mechanical properties are affected negatively by the addition of microcapsules, the composite matrices were found to have increased stiffness. This is evident from fracture toughness values increasing with increasing percentage of microencapsulate additions [14,18,19]. This increase of stiffness was observed regardless of the size of the microcapsules used. Smaller microcapsules exhibited higher stiffness at lower volume fractions (up to 10%). At higher volume fractions (>20%), regardless of the size of the microcapsules, the measured fracture toughness peaks reach an equivalent plateau [14]. In another study [20], it was reported that a high concentration of microcapsules increased the viscosity of the epoxy composite substantially during manufacture; however no specific data was provided. Similarly, Koh et al. [21] showed that incorporation of large volume fractions of microcapsules (>25%) in paint coatings affect significantly their hardening time- extending it by almost 70%.

In terms of healing, the majority of published data report that larger volume fractions of small sized microcapsules are required for the same size of cracks to achieve same level of healing. Brown et al. [14] reported maximum healing efficiency using 180 μm microcapsules at 5% volume fraction, whereas for 50 μm microcap-

sules the maximum healing was reached at a concentration of 20%. Similar observations were made by other researchers [18,22–24]. However, the percentage and type of catalysts used as well as the mechanical properties of the host matrix play an important role in the observed healing efficiency [25–27].

In the field of construction materials, the concept of introducing microcapsules for self-healing is relatively new. The earliest reported studies were conducted by Pelletier and Bose [28] and Yang et al. [29] for the production of self-healing concrete, while more recently the development of microcapsules for use in bituminous materials was also reported [30]. Following from the scarcity of data in the field of polymers on the effect of microcapsules addition, one can understand that the lack of such data in the field of construction materials is more pronounced. The vast majority of articles in the field mainly deal with production methods, characterisation and survivability issues and in the best case report some preliminary healing results. Pelletier et al. [31] in their proposed system of polyurethane microcapsules, ranging from 40 μm to 800 μm , reported a reduction of 12% in compressive strength of mortars containing 2% of microcapsules. In terms of toughness, they report negligible change while the observed healing, by means of load recovery, reached 24% compared to 12% of the control samples. Gilford et al. [32] reported that urea-formaldehyde microcapsules, with diameters in the range of 400 μm , at a volume fraction of 5% do not alter the modulus of elasticity. However, when the microcapsule concentration reduced to 2.5% and 1% inexplicably the modulus of elasticity dropped by 21% and 27% respectively. On another study using double-walled polyurethane/urea-formaldehyde (PU/UF) microcapsules, encapsulating sodium silicate, it was found that 2.5% addition of microcapsules increased the modulus of elasticity by \sim 14% [33]. In the same study when microcapsule concentration was doubled the modulus of elasticity dropped by \sim 5%, compared to the control samples. The modulus in this instance was measured using ultrasonic p-wave velocity. Mostavi et al. [33] also reported maximum healing efficiency, by means of crack depth measurements, 24% and 35% for microcapsules concentration of 2.5% and 5% respectively. The original crack depths in this study varied from \sim 78 mm for specimens with 2.5% microcapsules to \sim 88 mm and \sim 90 mm for samples with no microcapsules and 5% microcapsules respectively.

Wang et al. [34] examined the effect of UF microcapsules, added up to 9% by cement weight, on the mechanical properties of mortars. Their findings suggest that there was no significant change in compressive and flexural strength up to 6% addition of microcapsules. However, at 9%, a reduction of 35% and 25% was observed for compressive and flexural strength respectively. In terms of healing efficiency, the epoxy-carrying microcapsules exhibit their best performance at 9% reaching almost 100%. Healing efficiency in this case was measured in terms of load recovery as well as reduction in chloride permeability. J.Y. Wang et al. [35] embedded in mortar different percentages, up to 5%, of melamine formaldehyde microcapsules containing bacteria. The reported results show a significant reduction on both tensile and compressive strengths for the first 28 days. The reduction for both properties was gradual with increasing percentage of microcapsules and reached 25% and 34% for tensile and compressive strength respectively. J.Y. Wang et al. [35] also reported that after three months of curing the observed difference on the tensile strength was not statistically significant, whereas the difference on the compressive strength was increased further to 47%. In this work, the effect of the addition of microcapsules on the produced heat of hydration was also investigated. The results showed that the cumulative heat production was very similar when comparing the control mix with mixes containing 3% and 5% of microcapsules.

From the above discussion it is obvious that only a very limited number of studies have dealt with the effect of different

percentages of microcapsules on the properties of the composite. In addition, in the vast majority of these studies, the percentages considered are typically up to 5% with respect to cement weight. Moreover, the published data so far is either limited, contradicting or concerning only a restricted number of properties. In this study, the effect of polymeric microcapsules, carrying liquid sodium silicate, was investigated on both fresh (viscosity and setting time) and hardened properties (modulus of elasticity, compressive and flexural strengths). Furthermore, the healing potential of the investigated microcapsules under two different crack sizes was investigated. The microcapsules were added at various concentrations up to 32% by volume of cement. The potential of liquid sodium silicate as a suitable encapsulated healing compound in cementitious materials was discussed in a previous study [36].

2. Materials and preparation

The effect of the different volume fractions of polymeric microcapsules on the fresh, hardened and self-healing properties was investigated using mortar mixes. The mortars were prepared using ordinary Portland cement (CEM-I, 52.5N) and locally sourced fine sand, with maximum aggregate size of 1 mm. The sand-to-cement and the water-to-cement ratios were kept constant at 1.5 and 0.4 respectively for all mixtures. Prior to mixing, the microcapsules were removed from their storage containers, washed and vacuum filtered to remove the preservative liquid. Table 1 summarises the characteristics of the polymeric microcapsules used in this study. The microcapsules were manufactured in collaboration with our industrial partner Lambson Ltd. Table 2 presents rheological properties of the cargo material and Table 3 shows the corresponding microcapsule concentrations used in this study with respect to cement volume, cement weight and total mix weight.

Table 1
Characteristics of the microcapsules used in this study.

Shell Material	Cargo	Average size	Density	Average cargo volume per microcapsule
Pig Gelatine/ Gum Acacia	54% Mineral Oil 42% Sodium Silicate 4% Emulsifier Range	290 μm 98–632 μm	~ 0.98 g/cm^3	$\sim 0.014 \text{ mm}^3$

Preservative system: Phenoxy Ethanol/Sodium Benzoate/Dehydro-Acetic Acid/Xanthan Gum.

Table 2
Viscosity values of the various components used for cargo material at 20 °C.

	Viscosity (cps) ^a
Sodium silicate (SS)	37
Mineral oil (MO)	70
Cargo Material (43% SS + 54% MO)	44

^a Note: Viscosity values at 20 °C. Water viscosity at 20 °C is 1cp.

Table 3
Equivalent percentages for microcapsules addition for each reference quantity.

Microcapsules% addition with respect to:		
Cement volume (V_f)	Cement weight (Cwt)	Total mix weight (Twt)
4%	0.79%	0.46%
8%	1.57%	0.91%
12%	2.34%	1.36%
16%	3.09%	1.81%
24%	4.57%	2.68%
32%	6.00%	3.55%

The mixtures were prepared using a rotating pan mixer. The production started by dry mixing cement and sand for three minutes. The polymeric microcapsules were dispersed in the water of the mix to ensure better dispersion and distribution during mixing. Once dry mixing was completed, the solution of water and microcapsules was added in three parts into the mixer. Each part was followed by two minutes of mixing. Following the completion of mixing the material was moulded in prisms ($40 \times 40 \times 160 \text{ mm}$), cubes ($100 \times 100 \text{ mm}$) and cylinders ($\text{Ø}100 \times 200 \text{ mm}$) necessary for the experimental work. A mild steel wire of 1.6 mm in diameter was used in prisms to prevent catastrophic separation of samples during and after loading. The wire was placed at the top half of the specimens with a cover of 10 mm from the casting surface. Specimens were compacted using an electric motor vibration table and covered with a plastic film to reduce water loss. Samples were taken out of the moulds after 24 h and then stored in water ($20 \text{ °C} \pm 1 \text{ °C}$) for seven days. On the seventh day the relevant mechanical tests were performed and the samples designated to self-heal were returned to water for further 28 days. In all experimental procedures triplicates were used, unless otherwise stated. The only exception was for the Young's modulus measurements where only one cylinder per mix was tested as required by the relevant standard [37].

3. Experimental methods

3.1. Fresh properties

3.1.1. Rheological measurements

Typically, the addition of microcapsules into cement-based materials is investigated with respect to their effect on mechanical properties and healing efficiency. At the same time, their effect on rheological properties, and hence the workability, of the fresh mix is largely overlooked. A Brookfield DV3T Rheometer was used to measure the viscosity of mixes. For better understanding of the effect of microcapsules on the fresh properties, only cement paste was considered in viscosity measurements. Samples were prepared by mixing cement (CEM-I, 52.5N) with water and microcapsules for three minutes in a 10lt planetary type mixer. When the mixing was completed, 10 ml were inserted into the rheometer sample cup. A SC4-27 spindle was inserted before leaving the sample to settle for five minutes (Fig. 1).

After five minutes of resting time, pre-shearing from 0 to 30 s^{-1} was carried out for one minute to “erase” shear history due to mixing. The sample was then left still for 30 s to stabilise. After this, a shear stress vs. shear rate relationship was obtained by subjecting the sample to shear rates varying from 8.5 s^{-1} to 60 s^{-1} (ramp up) and back down to 8.5 s^{-1} (ramp down). The gradient of the linear

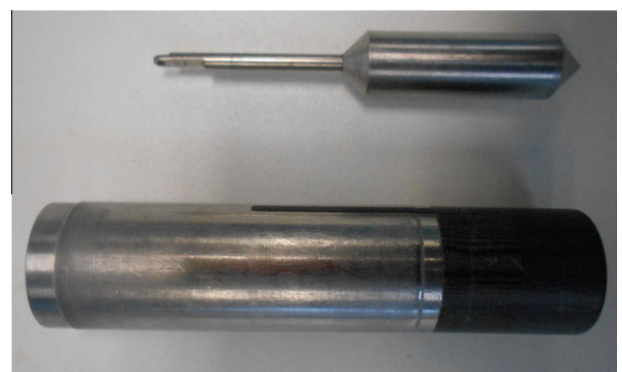


Fig. 1. The Brookfield SC4-27 spindle and corresponding sample cup used for the rheological measurements in this study.

regression of the ramp down portion of the shear stress vs. shear rate relationship was then used to obtain the viscosity.

3.1.2. Initial setting and heat of hydration

A Calmetrix I-Cal 2000 HPC High Precision Isothermal Calorimeter compliant with ASTM C1679 was used to measure the heat of hydration of the different mortar samples. The thermostat of the calorimeter was set to 23 °C and, after 24 h, the cement, sand, capsules and water were all pre-conditioned for two hours. After this time, the materials were mixed for one minute using a plastic spoon. Logging of the heat of hydration and the cumulative heat production was then carried out for 48 h. This time was sufficient to obtain the initial setting peak. The peak power is calculated as the maximum power (first peak) minus the power during the induction period (first trough). The initial setting time was then calculated as the time at one-third of the peak power.

3.2. Mechanical testing

3.2.1. Cracking of prisms

The mechanical loading of the prisms was performed on a 30 kN static testing frame. Prior to cracking, all specimens were notched with a rotating diamond blade. The notch depth and width were 1.5 and 2.0 mm respectively. A clip gauge was attached close to the notch edges to monitor crack mouth opening displacement (CMOD). The prisms were loaded over a span of 125 mm, at a rate of 0.125 mm/min and the loading was stopped when the crack opening reached the desired value. In this study, the effect of two different crack sizes on self-healing was also considered. For this purpose the prisms were divided in two categories and some were cracked at a maximum CMOD of 0.40 mm and some at CMOD of 0.5 mm. Upon load removal, the specimens with CMOD of 0.4 mm had residual crack widths in the range of 0.11–0.17 mm, whereas those loaded at a CMOD of 0.5 mm had residual crack widths in the range of 0.18–0.25 mm. Following cracking, the samples were then placed back into the curing bath for 28 days to facilitate the healing process. At the end of the healing period, prisms that would not be used in further experimentation (e.g. sorptivity measurements) were reloaded up to complete fracture. This led to the exposure of the inner crack faces and enabled the extraction of formed healing compounds for further microstructural analysis.

3.2.2. Compressive strength and modulus of elasticity

Compressive strength and modulus of elasticity measurements were performed on a 2000 kN servohydraulic compression frame using 100 × 100 mm cubic specimens and Ø100 × 200 mm cylinders. Both tests were carried out after seven days of specimen

casting in order to be consistent with the cracking age of the prisms.

3.3. Healing efficiency and characterisation

3.3.1. Crack area measurements

The bottom crack faces in all the specimens were monitored over time using a stereoscope. Digital images were captured at three different positions of the crack face, which were the same for all specimens. The cracks were photographed on the day of the cracking and at the end of the healing period at the exact same locations. Image analysis software (Image-J) was then used to analyse the acquired captions and the total crack area was calculated for each case. The crack area value obtained relates only to the two dimensional part of the crack that is visible by the stereoscope. The values obtained from the image analysis were used to calculate the crack mouth healing in each case using the following formula:

$$CMH(\%) = \frac{A_i - A_h}{A_i} \times 100 \quad (1)$$

where A_i is the crack area on the day of cracking and A_h is the area at the same point at the end of the healing period.

3.3.2. Ultrasonic measurements for crack depth and compressive strength

An ultrasonic measurement device was used for the determination of the crack depth for each prismatic sample following the guidelines in BS-1881: Part 203. The ultrasound probes are placed at specific locations adjacent to the crack as shown in Fig. 2. The time needed by the ultrasonic waves to travel from the two distinct points are recorded and the crack depth is calculated by Eq. (2):

$$d = X_i \sqrt{\frac{4t_1^2 - t_2^2}{t_2^2 - t_1^2}} \quad (2)$$

where d is the measured crack depth, X_i is the distance of the probes from the centre of the crack, t_1 and t_2 are times required by the ultrasonic waves to travel through the material from two different locations. In this instance the specimens were measured at the end of the 28 day healing period.

The same ultrasonic device and probes were also used to measure the ultrasonic pulse velocity on 28 days healed prism specimens. Using the correlation curve proposed by RILEM [38] the compressive strength of the material was estimated.

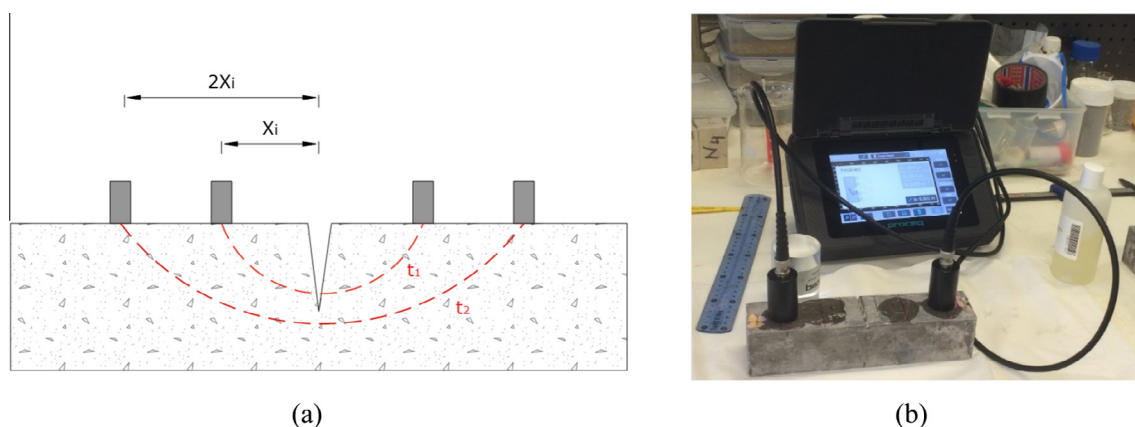


Fig. 2. (a) The principle of crack depth measurement using ultrasonic probes and (b) the crack depth measurements in the laboratory.

3.3.3. Liquid capillary absorption coefficient

The liquid capillary absorption coefficient was obtained for all prisms used in this study. At the end of the healing period the samples were removed from their water bath and placed in the oven at 40 °C for 72 h to remove moisture. Then, the bottom and side faces of the prisms were covered with insulating adhesive aluminium tape leaving only the crack area exposed. By doing this, it was made sure that the capillary absorption took place only by the crack itself. Weight changes of the specimens due to capillary suction were monitored for 4 h and 16 min in all specimens. The water suction quantity per unit area M_w is proportional to the square root of absorption time t according to [39]:

$$M_w = S\sqrt{t} \quad (3)$$

where S is the sorptivity coefficient of concrete, regressed as the slope of the curve between M_w and the square root of time.

3.3.4. SEM-EDX analysis

The SEM-EDX analysis was performed using a Nova nanoSEM 450 equipped with a Bruker Quantax Xflash 6/100 EDX detector. For SEM-EDX investigation small chipped pieces were extracted from the crack faces, coated with platinum and examined under a 10 kV accelerating voltage.

3.3.5. Optical and fluorescent microscopy

To verify that the microcapsules survived mixing and ruptured upon cracking, extracted chips from fractured cube surfaces were examined microscopically. For this purpose a Leica DM2700 upright optical microscope with an attached fluorescent cube was used.

4. Results and discussion

4.1. Viscosity changes with addition of microcapsules

Fig. 3 illustrates the viscosity variation of the cement paste as a function of the microcapsule concentration percentage.

It can be seen that gradual addition of microcapsules increased the measured viscosity of the cement paste. At 4% concentration the viscosity increase is only 11% and gradually increased by 36% at a concentration of 12%. However, at 16% concentration it seems that the mix reaches a critical point and the viscosity increases rapidly, reaching a maximum of more than 200% increase for concentrations above 24%. This finding is in a good agreement with previous published work on the effect of solid spherical inclusions in concentrated suspensions [40,41]. For a dilute phase, where the concentration of particles is low, the relative motion of fluid near and around

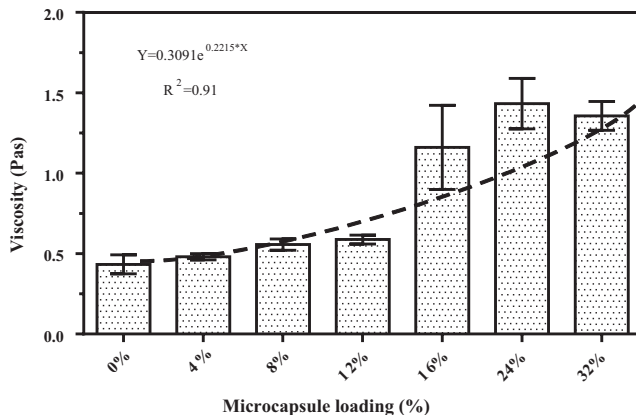


Fig. 3. Viscosity variation with increasing loading percentage of microcapsules with respect to cement volume.

them remains largely unaffected by the volume fraction of particles. For such dilute phases, Einstein had found that their viscosity is correlated linearly with increasing particle concentration [42]. Indeed, in this case for microcapsules concentrations below 12% the linear correlation is very strong with R^2 values reaching 0.98 whereas beyond 12%, the viscosity increases exponentially.

As the volume fraction of particles increases it creates the so-called *crowding* phenomenon. The increase in particles population obstructs the movement of fluid around them resulting in higher values of viscosity [40,43]. Moreover, when particles of different sizes are concerned, as in this case since the microcapsules are not monosized, the effect on the viscosity is more pronounced. Particles with different effective volumes when crowded can result in dead fluid trapped between them resulting in rapid decrease of the flowability of the suspension [44]. These observations have been found valid for cement-based systems as well as other Bingham fluids [42,45] and can explain the deviation from linearity in this case when the microcapsule concentration was increased.

4.2. Initial setting times and heat of hydration

The power and the cumulative energy produced per gram of cement for the first 48 h are shown in Fig. 4.

From the above graph it can be seen that the setting time (~4 h) was observed to be identical for both mixes. There is small difference in the maximum measured power, but it is insignificant. These findings show that the inclusion of microcapsules even at their highest concentration (32% by cement volume) does not affect the hydration process. This has also been found to be the case for lower volume fraction of the same type, but larger, microcapsules [46]. In addition, the cumulative energy release was very similar for both mixes at the end of the 48 h period. This indicates that the degree of hydration of both samples was the same. These findings are in very good agreement with previous results reported in the literature for microencapsulated bacterial spores (~2–5 μm) added to cement paste [35].

4.3. Effect of microcapsules addition on mechanical properties

The effect of microcapsule addition on compressive strength and modulus of elasticity of mortar is shown in Fig. 5. As expected, and coherent with the literature, the incorporation of microcapsules into the mix reduced the compressive strength. However, up to 8% V_f (1.57% Cwt) concentration the effect on the compressive strength is negligible. This finding somewhat contradicts previously reported data [31,35] where for up to ~2% Cwt microcapsules the observed reduction in the compressive strength was 10–15%. As far as the effect on the mechanical properties is concerned, this discrepancy is likely due to the fact that these

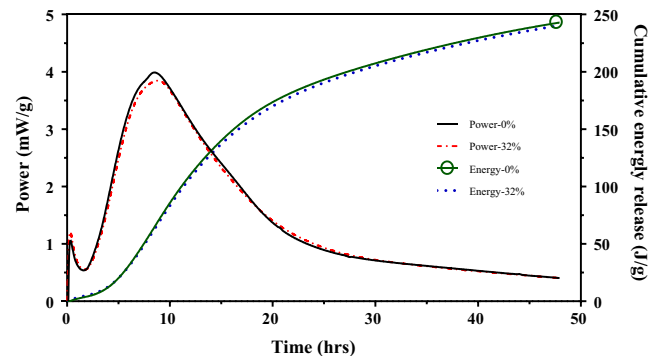


Fig. 4. Effect of maximum microcapsules concentration on isothermal (23 °C) power and energy production.

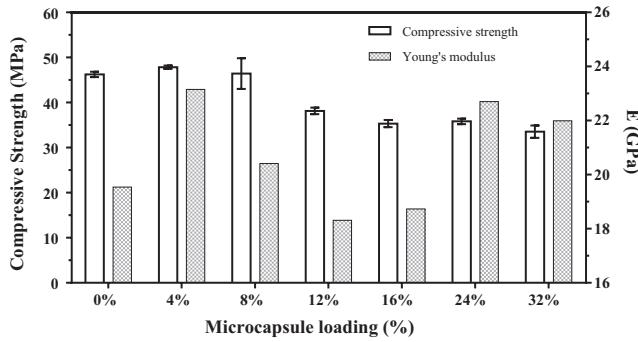


Fig. 5. Compressive strength and Young's modulus variation with increasing volume fraction (V_f) of microcapsules.

studies used either too large (up to 800 μm) [31] or too small (5 μm) [35] microcapsules. For similar sized microcapsules, as the ones used in this study, other researchers also report insignificant compressive strength changes at low percentages with respect to the cement weight [34].

The lowest volume fraction at which the effect of microcapsule addition becomes noticeably detrimental is at 12% V_f . At this point, the reduction in the compressive strength was $\sim 17\%$. Subsequently, regardless of the volume fraction used the reduction in the compressive strength reached a plateau in the range of 24–27%. However, since all mixes have been prepared and compacted in the same way it is not clear whether this reduction in strength is entirely due to the presence of the microcapsules within the hardened cementitious matrix or also due to their contribution in increasing the viscosity of the mix substantially. As far as the modulus of elasticity is concerned, the obtained results do not show a clear pattern on the effect of microcapsules. Interestingly the only two studies in this field that studied the effect of microcapsules on Young's modulus also reported similar fluctuations [32,33]. Compressive strength measurements were also performed using ultrasonic waves on the prisms at the end of the 28 days healing period (Fig. 6).

The ultrasonic measurements also showed a decreasing trend for the compressive strength with increasing volume fraction of microcapsules. Nonetheless, this reduction does not seem to be significant up to a concentration of 16%. The monitored reduction for the two largest volume fractions was 30% and 37% and is consistent with the observations from crushed cubes at 7 days. However, it is worth mentioning that ultrasound testing is an indirect, and thus less reliable, method of assessing strength. The correlation formulae between ultrasound pulse velocity and compressive strength are based on normal concrete, consisting of voids

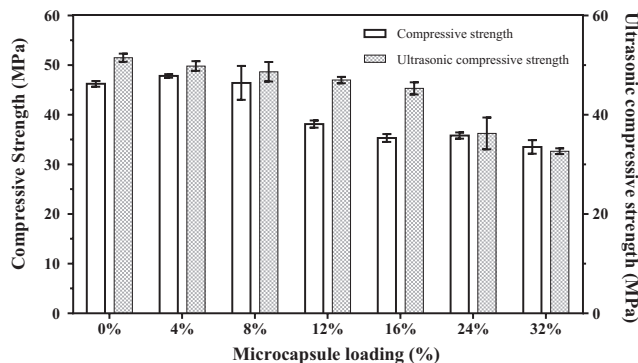


Fig. 6. Comparison of compressive strengths measured mechanically and using ultrasonic waves.

and a hard matrix. Microcapsules themselves will most likely provide improved ultrasound wave transmission when compared with air voids and this could also explain the overestimation of this approach for the vast majority of samples containing microcapsules. Fig. 7 shows the variation of the ultimate flexural strength and fracture toughness as obtained from three-point bending tests of prisms. Fracture toughness was calculated using:

$$K_{Ic} = \frac{P \times S}{W \times D^{3/2}} f\left(\frac{\alpha}{D}\right) \quad (4)$$

where P is the maximum load in flexure, S is the loading length, W and D are the specimen's width and depth and $f(\alpha/D)$ is a geometric function that correlates the crack depth (α) with the depth of the specimen.

It is clear that the addition of microcapsules to some extent has provided an increase in the strength and fracture toughness of the specimens. However, no significant changes are observed between the different volume fractions. Similarly, the incorporation of microcapsules has increased the fracture toughness. This increase reached 23% at a V_f of 12%. Increasing the microcapsule concentration resulted in a reduction of fracture toughness. This observation is consistent with reported data on similar size polymeric microcapsules embedded in epoxy matrices [14,19]. This observed anomaly has been identified in materials incorporating large volume fractions of embedded particles and is a result of the developing stress fields during cracking. When embedded spherical particles are densely packed at large volume fractions, the stress needed for crack propagation becomes very large. The crack is pinned at multiple locations and then tends to extend around the periphery of the particles, therefore debonding them, rather than extending between them by bowing outwards, and hence rupturing, them [47]. Furthermore, in this case, the considerable increase in the viscosity of the mix at large volume fractions is believed to enhance this phenomenon. Reduction in the fracture toughness is also attributed to the poor bonding between the embedded spherical particles and the host matrix [48,49]. The viscous nature of the mixes incorporating large volume fractions of microcapsules could potentially have led to poor compaction of the cement matrix and hence low levels of adhesion between the microcapsules and the cement paste.

4.4. Microscopic observations on cracked faces

Fig. 8 illustrates some typical microscopic images taken from chips extracted from fracture surfaces. The microcapsules used in this study fluoresce when exposed to ultra violet (UV) light and thus were easily distinguished from pores or sand particles. It has to be noted that the following images were taken on

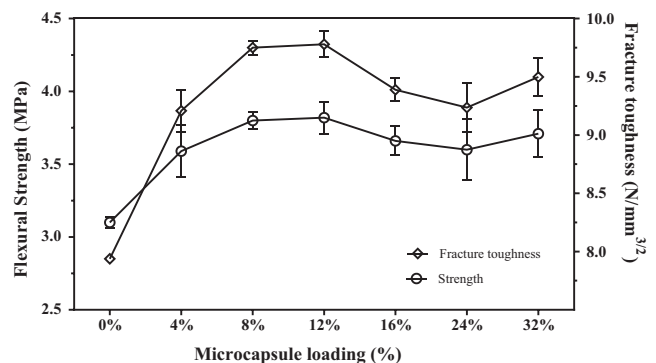


Fig. 7. Flexural strength and fracture toughness variation with increasing volume fraction (V_f) of microcapsules.

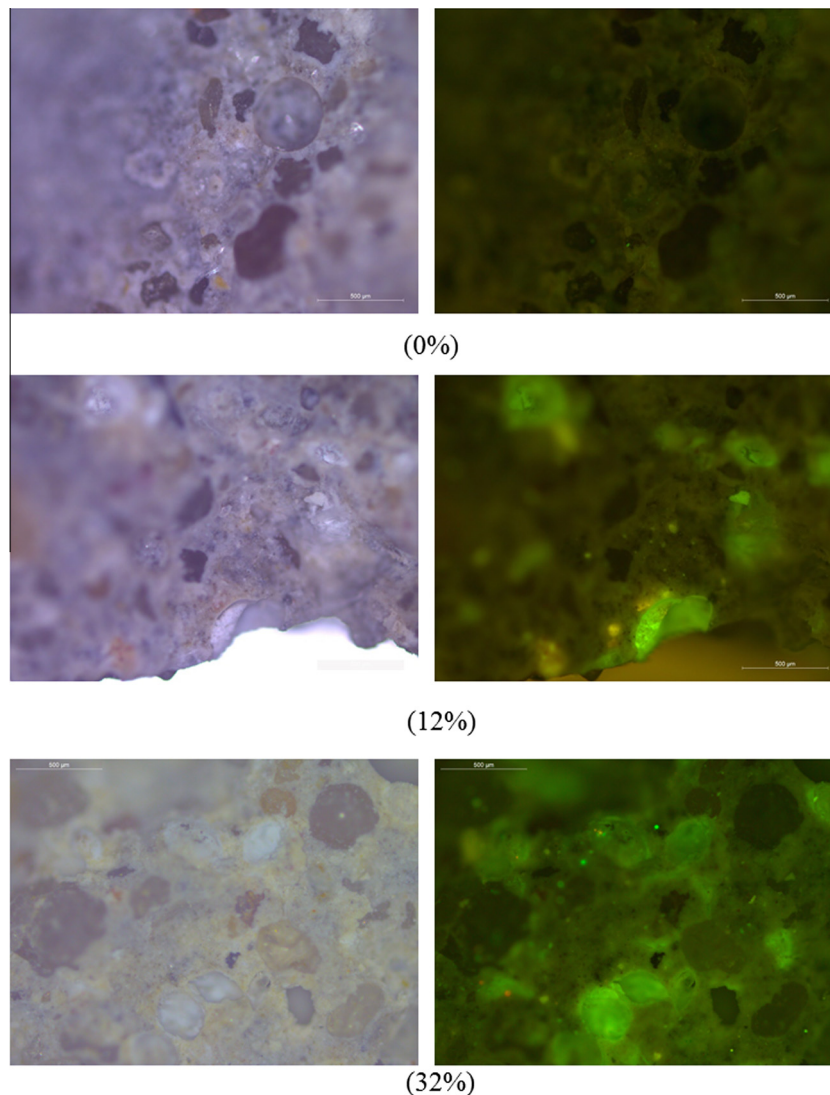


Fig. 8. Typical optical microscope images of fracture surfaces under visible light (left) and UV light (right) (Note: scale bars correspond to 500 μm).

unpolished non-flat surfaces, to avoid damaging the microcapsules. Therefore, they should be used for comparative purposes.

Optical microscope observations showed an increasing number of fractured microcapsules with increasing microcapsule concentration. This indirectly confirms that the microcapsules survived mixing and ruptured during crack formation. Further analysis of the microscopic images showed that, with increasing volume fraction, there is a tendency for the microcapsules to form agglomerations as observed in Fig. 9. For a given area of fracture surface, the number of microcapsules not only increases but it is clear that they form clusters. This finding verifies the earlier hypothesis that the coupling of large volume fractions and increased viscosity can result in densely packed and poorly dispersed particles.

Although compaction in cement-based materials reduces considerably the number of pores in the matrix their total elimination is not always possible, especially in the most common types of concrete. Pores are known for their detrimental effect on concrete's durability but their presence can be also problematic for self-healing if microcapsules are in close vicinity. The reason for this is that the contents of the microcapsules can be potentially consumed within the voids' volume without actually contributing towards healing the formed crack. As it can be observed these voids are of similar size to the microcapsules, and therefore the

0.014 m^3 (see Table 2) of cargo material carried by the microcapsules will not be sufficient to fill this space. Microscopic images revealed that there were cases where microcapsules either were very close or even ruptured on the tip of a pore (Fig. 10a). Microcapsules were also observed to be surrounded by a large number of aggregates (Fig. 10). This will result in limited healing as the encapsulated sodium silicate will not interact chemically with the aggregates as strongly as it interacts with the cement hydration products.

4.5. Crack healing

4.5.1. Crack mouth closure

Stereoscope images of the bottom crack mouth opening showed the process of healing at the end of 28 days (Fig. 11).

As it can be clearly observed for the samples with microcapsules, the cracks have been almost completely healed after 28 days. The total crack mouth healing for both types of samples is shown in Fig. 12.

All specimens containing microcapsules have healed better compared to the control samples regardless of the CMOD level. Although the residual crack ranges may not seem excessively large the damage caused to a specimen of this size when loaded to

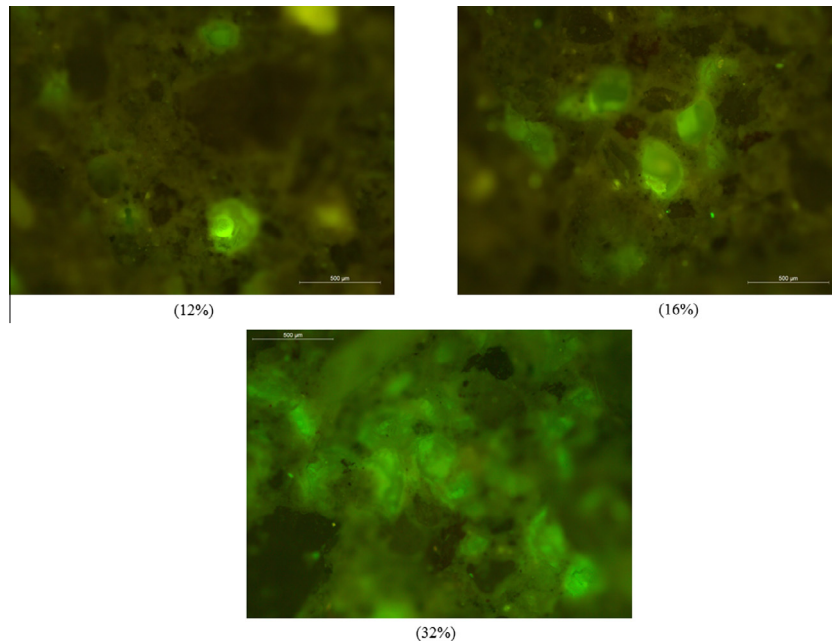


Fig. 9. Increased agglomeration of microcapsules with increasing volume fraction (Note: scale bars correspond to 500 μm).

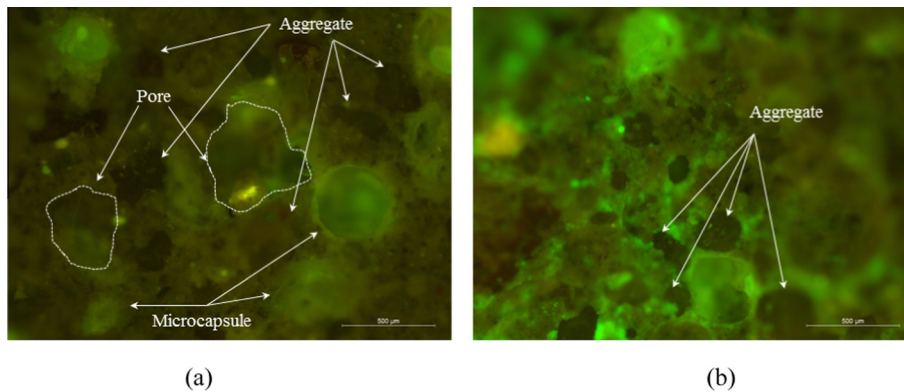


Fig. 10. Microcapsules located close to: (a) large pores and (b) aggregates (Note: scale bars correspond to 500 μm).

CMODs of 0.4 and 0.5 mm is substantial. The residual crack opening is undeniably very important but the crack depth, which is strongly associated with initial crack level, is equally a major factor in the overall healing process. The addition of microcapsules assisted the healing process considerably and resulted in an improvement in the crack mouth healing from 20% up to 77%. Increasing the size of the crack during loading resulted in consistently lower healing percentages for all samples. In addition, the specimens cracked at larger CMOD had also larger spread in the obtained crack mouth healing values compared with the values for samples loaded at a smaller crack. For such large initial crack opening it was noticed that small fracture debris, of either the matrix or the sand, could roll and bridge across the crack (Fig. 13a). This potentially could affect the level of healing since fracture debris is not a stable scaffold for the proliferation of formed healing products. Moreover, it was noticed that accumulation of large aggregate particles near the crack mouth also resulted in lower levels of healing (Fig. 13b).

The healing products that formed at the crack mouth mainly consist of healing products produced due to the fracture of the microcapsules. The released sodium silicate solution interacts chemically with the cementitious matrix producing an excess of

hydration products [36]. In addition, carbonation crystals due to the autogenous healing of the cementitious matrix were also deposited at the crack mouth.

Normalised crack mouth healing results are shown in Fig. 14. Normalised crack mouth healing was calculated by subtracting the contribution of autogenous healing, which is the healing values of the control group, from the values of the samples containing microcapsules. The results show that the effect of microcapsule addition on healing is, in most cases, similar regardless of the size of the initial crack. However, the larger the initial crack, the larger the damage to the cementitious matrix and hence the lower the level of the autogenous healing. This, in combination with fracture debris existing in larger cracks, led to the observed differences shown in Fig. 12 even though the impact of microcapsules is comparatively the same for most volume fractions.

4.5.2. Crack depth measurements

The effect of the level of damage on the healing process was also evident in the ultrasonic measurements for the crack depth (Fig. 15).

The measured crack depths for control samples damaged to a CMOD of 0.5 mm showed cracks extending very deep into the

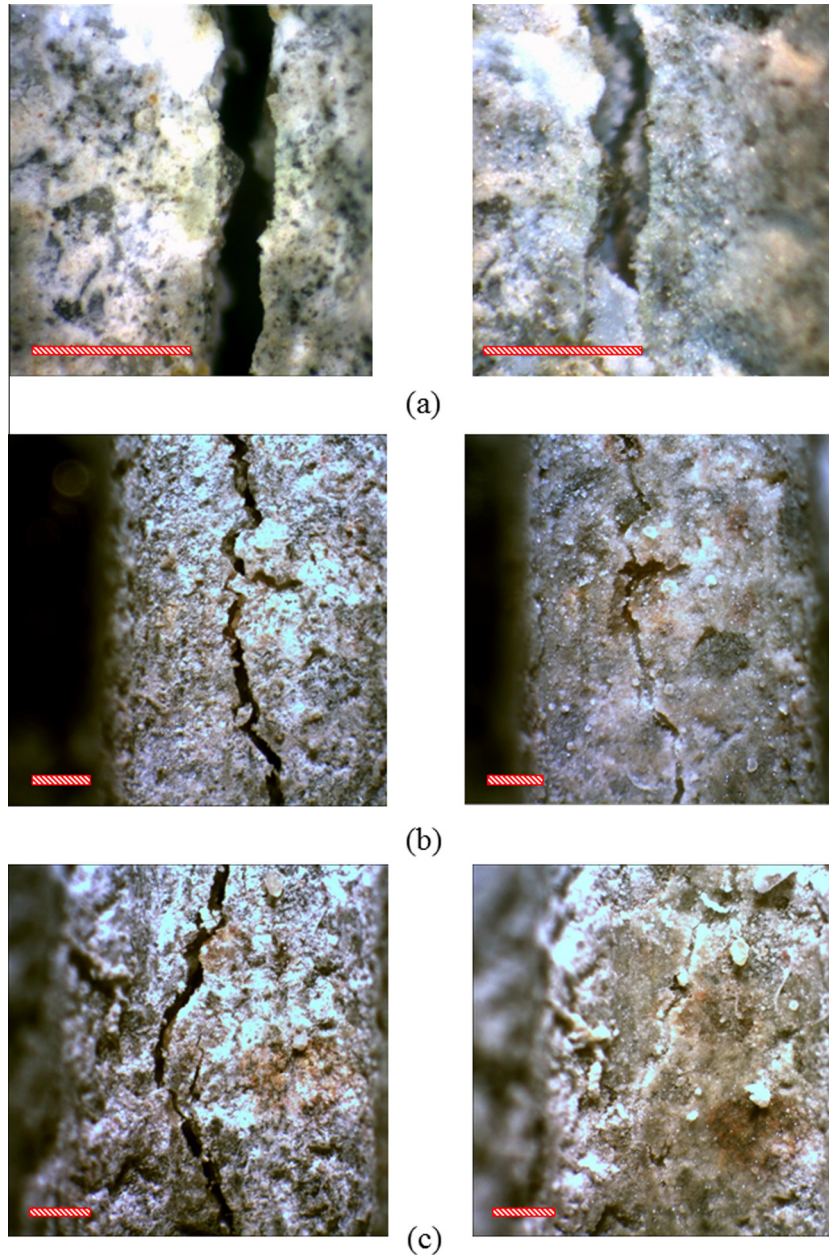


Fig. 11. Typical digital stereoscope images of crack mouth taken on the day of cracking (left) and after 28 days of healing (right) for: (a) control samples with no microcapsules; (b) sample with a V_f of microcapsules of 24% and (c) with a V_f of 32% (Note: solid bars correspond to 500 μm).

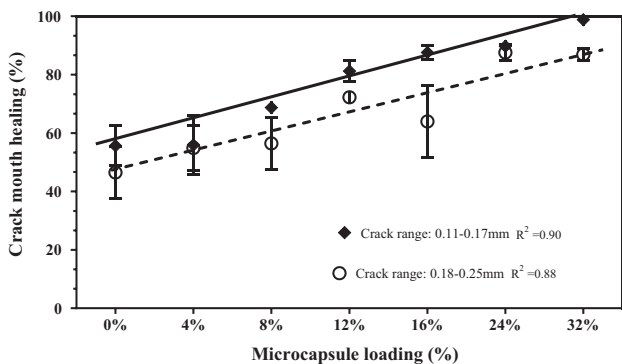


Fig. 12. Crack mouth healing (%), after 28 days, with respect to microcapsules volume fraction (V_f) for samples cracked at two different crack ranges: 0.11–0.17 mm (CMOD = 0.4 mm) and 0.18–0.25 mm (CMOD = 0.5 mm).

section reaching almost the top face. Even after 28 days of healing the crack depths remained relatively large for both types of control samples. For samples fractured at smaller initial crack a progressive trend in the reduction of crack depth with increasing concentration of microcapsules was observed. For larger cracks, although there is a substantial reduction in the crack depth, it appears that there is no significant change between 8 and 16% V_f . It seems that the damage in the cementitious matrix is too extensive and a greater volume fraction of microcapsules is required to reduce the crack further.

Combining results from crack mouth healing and the ultrasonic measurements of the crack depth a strong relationship is observed (Fig. 16). The crack mouth healing is linearly correlated with the reduction in crack depth. In fact, this correlation is stronger in the case of samples loaded at a CMOD of 0.4 mm (Fig. 16a). This reinforces the idea that the damage in the specimens loaded at a CMOD of 0.5 mm is so large that the information provided by

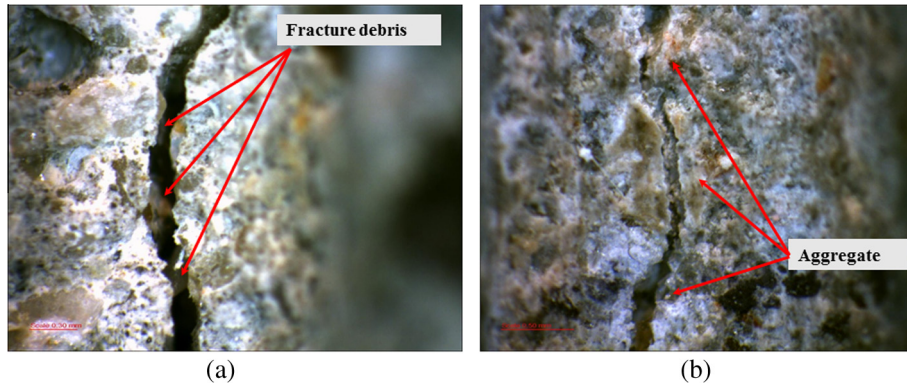


Fig. 13. Digital stereoscope images of the crack mouth showing: (a) fracture debris bridging across large cracks and (b) low level of healing in the vicinity of large aggregates.

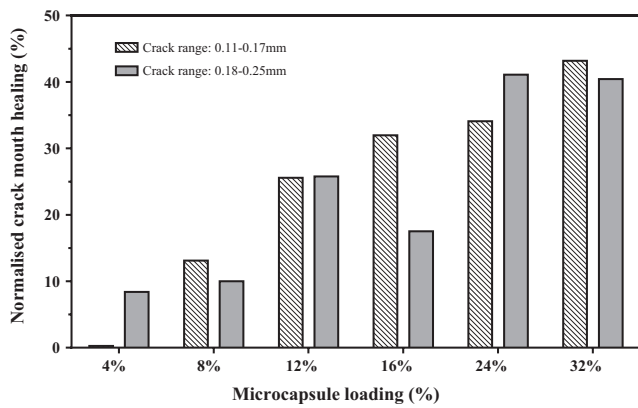


Fig. 14. Normalised crack mouth healing (%) at 28 days for different volume fractions of microcapsules at two different initial cracking levels.

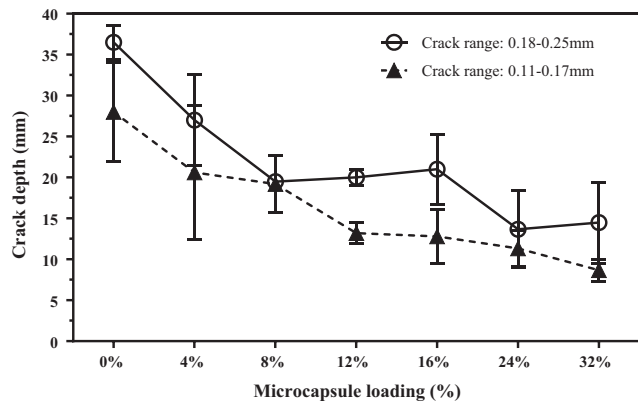


Fig. 15. Crack depth variation with increasing volume fraction of microcapsules for two initial cracking levels.

visual observation of the crack mouth (Fig. 12) is not representative of the healing that actually takes place deep inside the crack. On the other hand, for smaller initial cracks, it seems that the visual observations of the crack mouth can be regarded as a good indication of the overall healing. Nonetheless, it has to be highlighted that even for the smaller crack range the ultrasonic measurements revealed some residual crack depth (~8.6 mm) for the dosage of 32% of microcapsules that visually showed 100% crack mouth healing.

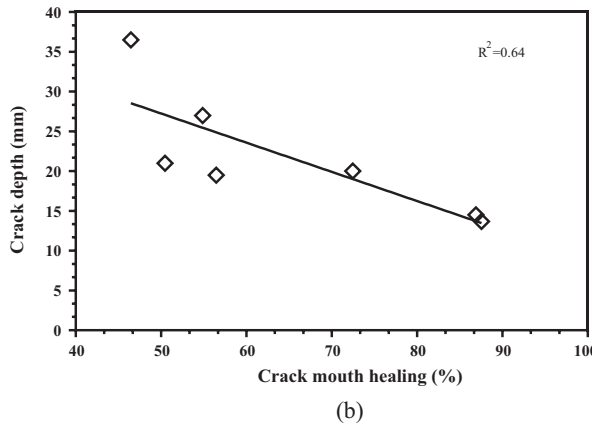
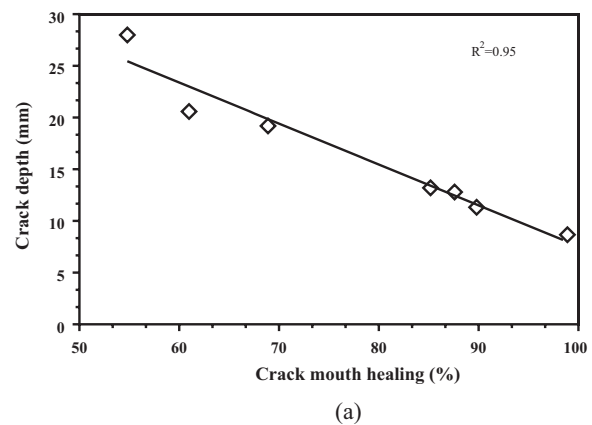


Fig. 16. Correlation between crack depth and observed crack mouth healing for: (a) samples with cracks range 0.11–0.17 mm (CMOD of 0.4 mm) and (b) samples with cracks range of 0.18–0.25 mm (CMOD of 0.5 mm).

4.6. Capillary absorption coefficient

Sorptivity measurements were taken only for samples initially cracked to a CMOD of 0.4 mm. Fig. 17 shows the calculated sorptivity coefficients for all cracked samples with varying concentration of microcapsules. For comparative purposes, the sorptivity of an uncracked sample for each mix was tested to highlight the difference between the two states (cracked/uncracked). Even after 28 days of healing, cracking resulted in a considerable increase in the sorptivity coefficient of mortar samples. This increase was more evident in the control samples where sorptivity increased by almost one order of magnitude.

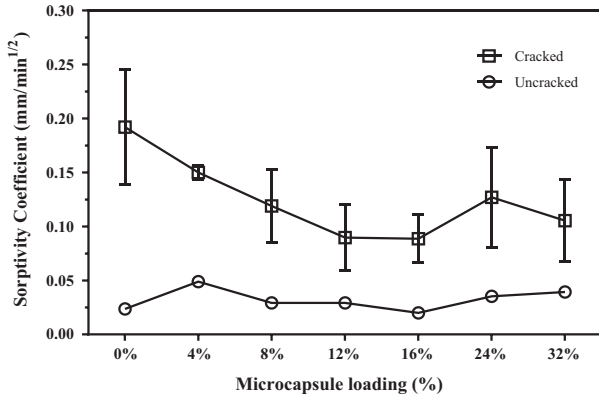


Fig. 17. Measured sorptivity coefficients with increasing concentration of microcapsules for cracked and uncracked samples.

With respect to the cracked samples, it is obvious that the use of microcapsules reduced substantially the measured sorptivity coefficients. This improvement maximised at 16% volume fraction of microcapsules which showed a 54% reduction in the sorptivity coefficient with respect to the control samples. Practically this means that the control samples absorb almost two times more water than the corresponding samples containing 16% microcapsules. The water uptake for each mix is shown clearer in Fig. 18.

The significant reduction in the water absorption is a strong indication that the life expectancy of the cracked sections containing microcapsules will be substantially improved compared to the non-containing ones. The observed initial trend of continuous sorptivity reduction with increasing volume fraction of microcapsules did not continue for the two largest volume fractions. The explanation for this inconsistency is twofold. As shown visually earlier, at these large volume fractions the microcapsules showed the tendency to coalesce forming clusters. In addition, the space occupied by the microcapsules can be considered as a pore or as a discontinuity. This, coupled with the ability for the shell material to absorb water and swell, could be the reason for the increased sorptivity values compared with the corresponding values from smaller volume fractions. Moreover, while plotting the cumulative volume absorbed versus time, in order to calculate the sorptivity coefficients, a behaviour characteristic to layered materials was exposed (Fig. 19). The water capillary sorption into the healed samples containing microcapsules did not take place at a constant rate as it would happen in a homogenous non-layered material [50].

The above pattern was characteristic to the vast majority of measurements for healed cracks. In these cases, slightly after the start of the test the slope of the graph decreased dramatically. This suggests that the wet front came into contact with a phase of lower

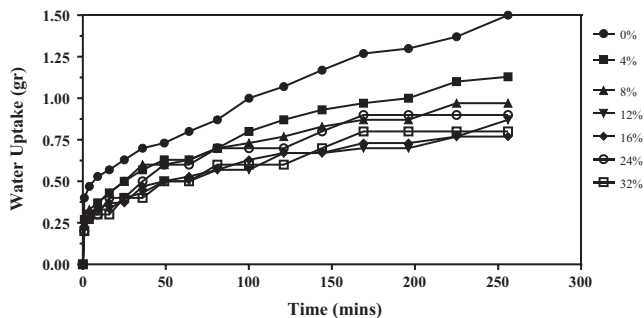


Fig. 18. Measured water uptake during sorptivity testing for cracked samples (CMOD = 0.4 mm).

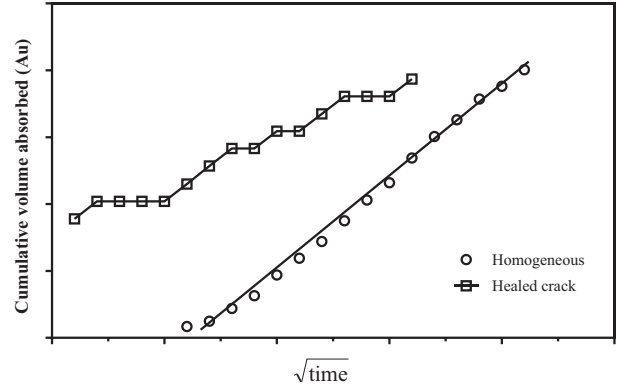


Fig. 19. A typical example of cumulative volume absorbed (in Arbitrary Units) with respect to time for a homogenous uncracked mortar sample and for a healed crack.

sorptivity. As the capillary absorbance continued, the water penetrated through a lower sorptivity region into a higher one and the slope increased again. The same pattern continued until the end of the test. This is an indication that the compounds filling the crack are layered and not homogenous. Moreover, this shows that there are sorptivity gradients within the crack. The lower sorptivity layers can be attributed to the formation of the healing products. This was also confirmed by the overall reduction in the measured sorptivity coefficients for all samples containing microcapsules. On the other hand, the higher sorptivity layers can be areas where either the healing products have not formed properly or may be areas with uncracked microcapsules.

Sorptivity values show a relatively good linear correlation with crack mouth healing values and crack depth measurements (Fig. 20).

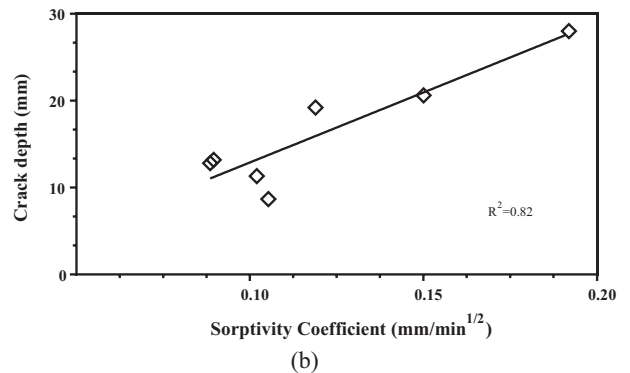
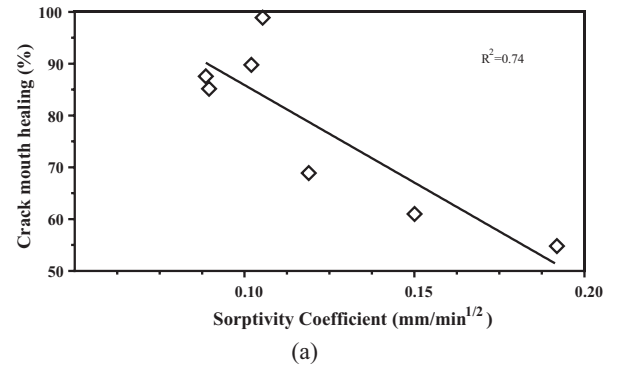


Fig. 20. Sorptivity correlation with: (a) crack mouth healing and (b) crack depth measurements.

4.7. SEM and EDX elemental analysis

SEM images revealed that the matrix's hydration products have created a series of "connecting rods" that mechanically lock the microcapsules in position (Fig. 21).

Elemental analysis showed that the connecting compounds between the microcapsules and host matrix are mainly ettringite and calcium silicate hydrates (C-S-H). This means that hydration near and around the polymeric shell was not affected and therefore unfavourable interactions had not taken place. A very common

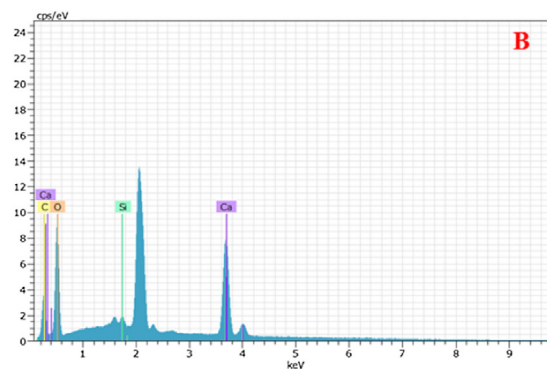
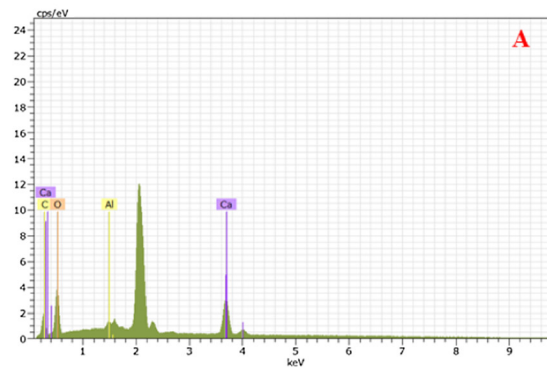
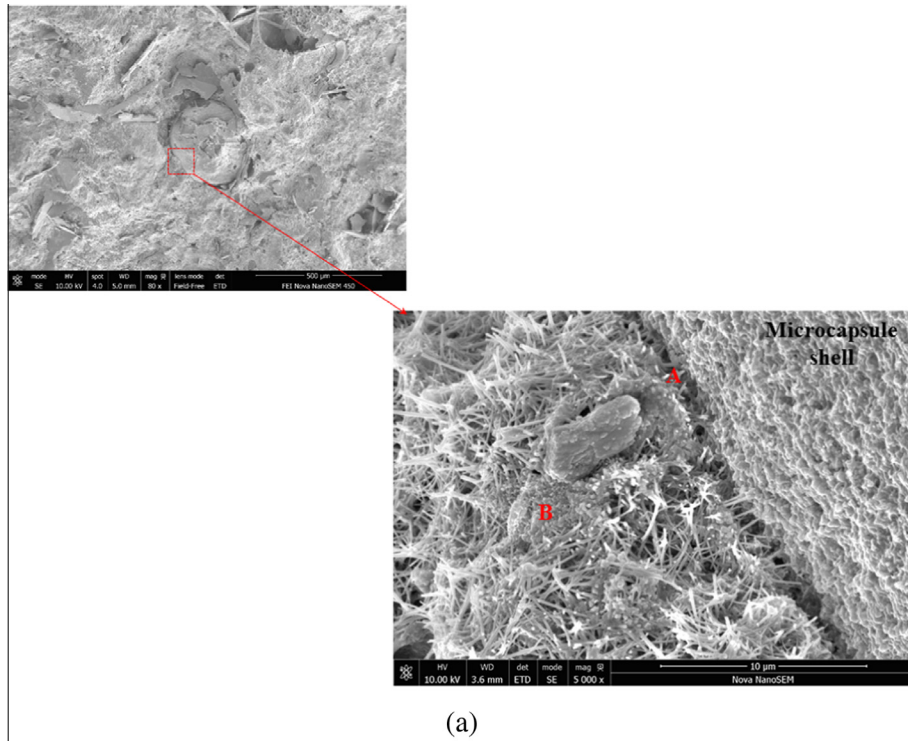


Fig. 21. (a) SEM image of the interface between the embedded microcapsule and the surrounding cementitious matrix and (b) EDX elemental analysis at the point of contact between the microcapsule and the matrix (point A) and at a neighbouring location (point B).

pattern observed in all samples containing microcapsules was their tendency to attract microcracks (Fig. 22).

In the vast majority of cases this attraction resulted in the deflection of the crack path and the formation of microcracks. Black arrows on Fig. 22 indicate the crack paths for each case, whereas the schematic illustrates the concept. This is very important since it shows that the microcapsules not only remained firmly embedded within the cementitious matrix, but also attracted cracks and ruptured when needed. In addition it also indicates the good bond between the microcapsules and the matrix. A weaker bond would have resulted in crack bowing and hence delamination and debonding of the microcapsules. However, in this case increased stress levels were required to overcome the bond strength. These in turn resulted in the rupture of the polymeric shell, the deflection of the crack path and the formation of microcracks on the opposite side of the initial crack front. This process can also explain the observed toughened nature of the samples containing microcapsules (Fig. 7).

Nonetheless, microcapsule delamination and poor bonding with the cementitious matrix was observed for samples from the two largest volume fractions (24% and 32%). Fig. 23 shows two typical

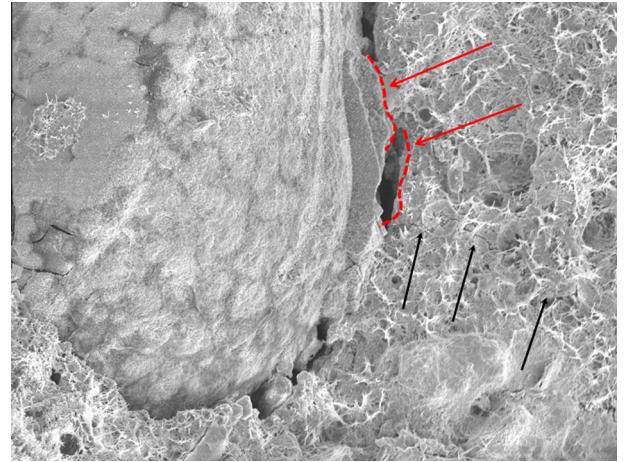


Fig. 24. Close up image of a debonded microcapsule; black arrows indicate the microcrack close to the capsule and red arrows show the fractured bonding material. (For interpretation of the references to colour in this figure legend, the reader is referred to the web version of this article.)

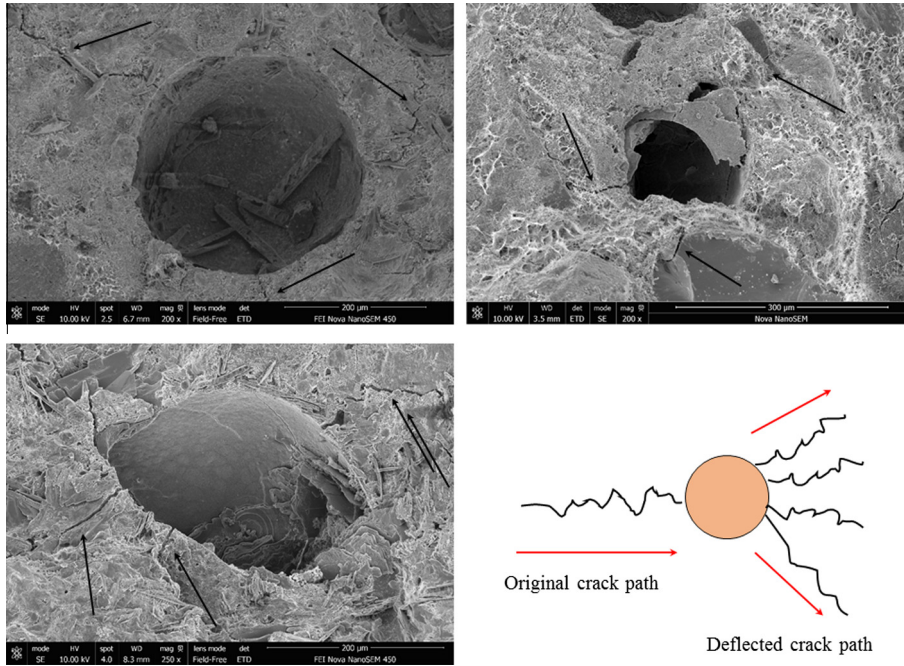


Fig. 22. SEM images showing the crack propagation and deflection pattern around the microcapsules.

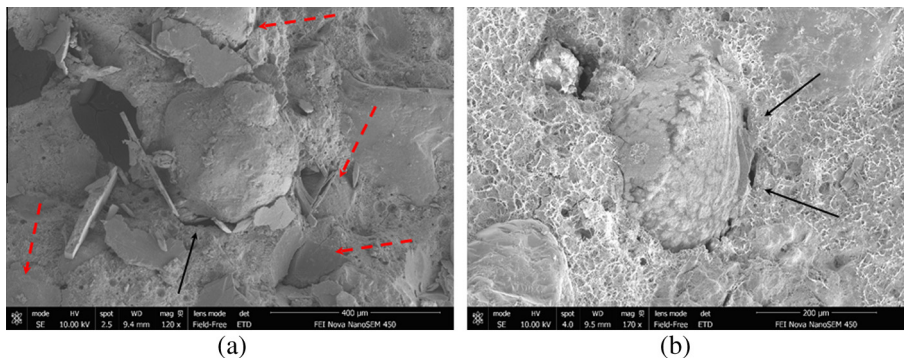


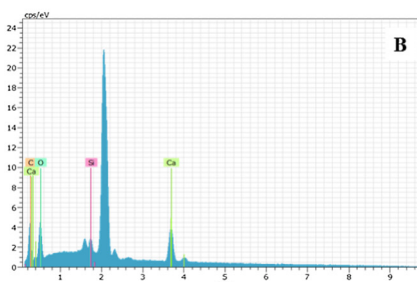
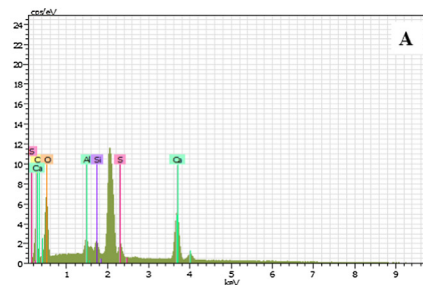
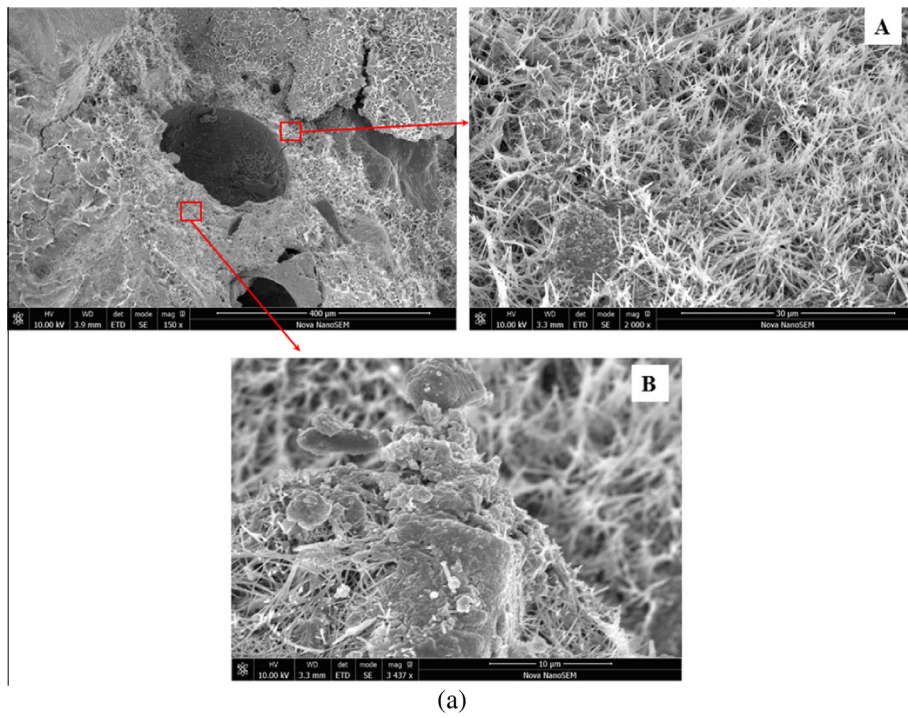
Fig. 23. SEM images delaminated and poorly bonded microcapsules; black solid arrows show the delamination area and red dashed arrows show locations of other microcapsules. (For interpretation of the references to colour in this figure legend, the reader is referred to the web version of this article.)

cases of poor bonding and delamination of microcapsules. The solid black arrows outline the delaminated region whereas red dashed arrows point to locations where other microcapsules are located.

Since samples have undergone 28 days of healing at this point is not possible to identify with certainty whether the delamination took place during cracking or it was the result of cavitation due to poor compaction during casting. However, by closely inspecting the images, for example the image shown in Fig. 23b, microcracks are observed to form near the microcapsule (Fig. 24). In addition, the hydration products that connected the microcapsule to the matrix seem to have undergone fracture and delamination.

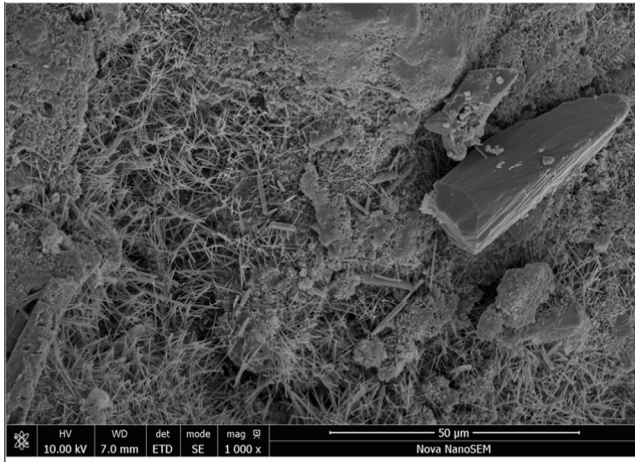
Similarly, fractured debris of hydration products appear in Fig. 23a as well. These observations lead to the conclusion that most probably the microcapsules debonded during cracking. This validates the earlier hypothesis which linked the bond quality with the increased viscosity values and the large number of particles at high volume fractions. Delamination of microcapsules resulted in lower stress levels which in turn explain the reduction in the fracture toughness for the large volume fractions.

Images and elemental analysis in the vicinity of fractured microcapsules revealed the formation of different hydration products (Fig. 25). The most dominant products were ettringite and CSH.

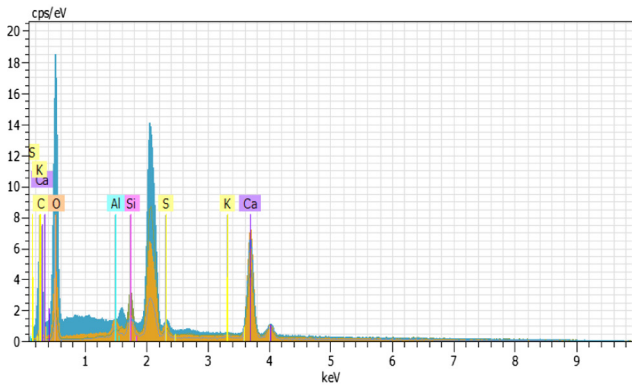


(b)

Fig. 25. (a) SEM images and (b) EDX elemental analysis of formed healing products in the close vicinity of a fractured microcapsule.



(a)



(b)

Fig. 26. (a) SEM image and (b) EDX elemental analysis of autogenously formed healing products in the control sample.

The areas in close proximity to the fractured microcapsules are generally dense with intense formation of crystalline and amorphous phases. In addition, in few occasions, sodium traces were also detected near the microcapsules. These observations confirmed that the cargo component was successfully released and reacted with the cementitious matrix producing a surplus of hydration products. Fig. 26 shows a SEM image and EDX elemental analysis from the reference sample (0% V_f of microcapsules).

Autogenously formed crystalline and amorphous phases create a network of hydration products, as observed before for the samples containing microcapsules. However, comparing Figs. 25a and 26a the packing of these products does not seem as dense as the packing of the formed products in the vicinity of ruptured microcapsules. Elemental analysis verified the formation of hydration phases like ettringite, calcium silicate hydrates and portlandite.

These formed healing products form a network of crystals that bridge across the cracks and eventually heal them. The denser the formed network, the better the healing. Moreover, it is obvious that the smaller the crack the more effective the healing is and this was confirmed by both crack mouth healing and crack depth measurements. Moving towards the mouth of the crack, the distance between the fractured planes becomes larger and as a result the bridging action of crystals becomes more difficult. This resulted in areas with inadequate bridging and therefore with higher sorptivity values. In addition, since the crack mouth was exposed more to the external environment (water in this case) this will promote greater formation of carbonate products and particle deposition. On the other hand, moving towards the tip of the crack, the distance of the crack planes become gradually smaller and the healing processes become more efficient. This is probably the explanation for the observations that on the one hand showed proper crack mouth healing (Fig. 12) but on the other hand revealed some residual crack depth (Fig. 15). The concept of the healing action provided by the embedded microcapsules is illustrated in Fig. 27.

For a limited number of samples, microcapsules that had broken during mixing and casting were noticed (Fig. 28). The

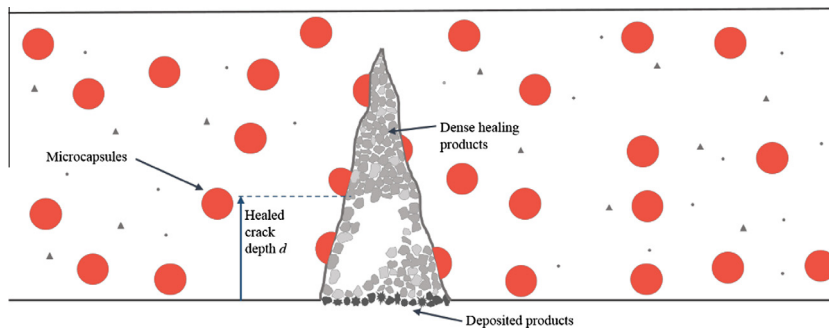


Fig. 27. Illustration of the healing process offered by embedded microcapsules in mortars (not to scale).

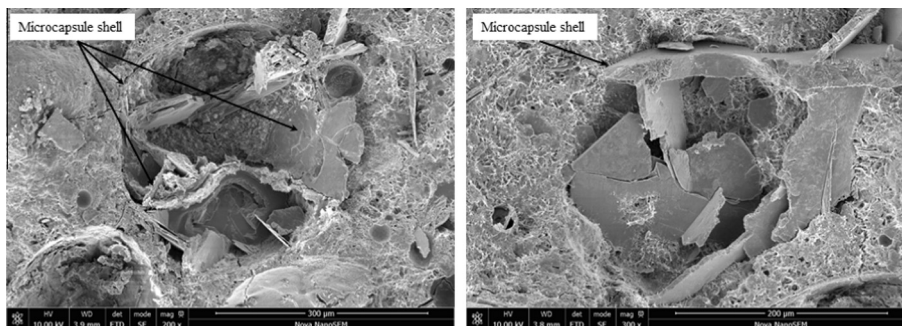


Fig. 28. SEM images showing microcapsules broken during mortar production and the hydration products that have developed in their nuclei.

microcapsules in this case have not retained their spherical shape and most of their shell was clearly destroyed. In addition, hydration products have developed in their nucleus.

5. Conclusions

This study has shown that microencapsulated sodium silicate solution can undoubtedly be successfully used for autonomic self-healing of cement-based materials. In addition, it demonstrated the effect of using a large spectrum of volume fractions of microcapsules on the fresh, mechanical and self-healing properties of mortars. The inclusion of microcapsules into the mix did not affect setting time and hydration but did have a substantial effect on the viscosity of the mix. The maximum increase in viscosity when compared to the control mix was more than 200%. Eventually, this affected the level and quality of compaction and hence the performance of the hardened material. The compressive strength, measured with two different techniques, showed a consistent decrease with increasing concentration of microcapsules. However, the reduction in both compressive strength and elastic modulus was substantially lower than the healing potential provided by the microcapsules. The healing levels as measured by crack mouth healing, crack depth measurements and sorptivity showed in all cases that the inclusion of microcapsules improved the crack closure and reduced the water absorption significantly. These findings were very consistent in samples initially fractured at small crack sizes (CMOD of 0.4 mm). Satisfactory healing was also observed in specimens with larger initial cracks (CMOD of 0.5 mm). Nonetheless, these samples had a constant lower self-healing performance and they were characterised by a relatively large scatter in the obtained results. Optical and scanning electron microscopy revealed that the vast majority of microcapsules survive mixing and rupture during cracking. However, in samples with a large volume of microcapsules, an agglomeration of microcapsules was observed and this could be the result of the increased viscosity in the mix.

In terms of optimum performance combining all the above discussed data a dosage of 16% volume fraction of microcapsules seem to be the most appropriate. Larger volume fractions (24% and 32%) were found to have slightly increased sorptivity coefficients with relatively large deviation in the results (Fig. 17). In addition, samples containing 24% and 32% V_f of microcapsules also showed indications of microcapsule debonding during crack development. Experimental evidence suggests that this behaviour can be the result of the increased viscosity in the matrix due to the high concentration of microcapsules.

Nonetheless, the use of viscosity modifying agents could provide a solution in successfully dispersing larger volume fractions of microcapsules hence leading in better performance. Moreover, an increase in the sodium silicate concentration in the microcapsules can potentially result in high self-healing levels at lower microencapsulate concentrations.

Acknowledgements

Financial support from the Engineering and Physical Sciences Research Council (EPSRC – United Kingdom) for this study (Project Ref. EP/K026631/1 – “Materials for Life”) is gratefully acknowledged.

Additional data related to this publication is available at the University of Cambridge's institutional data repository: <http://dx.doi.org/10.17863/CAM.321>.

References

- [1] S.R. White, N.R. Sottos, P.H. Geubelle, J.S. Moore, M.R. Kessler, S.R. Sriram, et al., Autonomic healing of polymer composites, *Nature* 409 (2001) 794–797.
- [2] C. Dry, Matrix cracking repair and filling using active and passive modes for smart timed release of chemicals from fibers into cement matrices, *Smart Mater. Struct.* 3 (1994) 118–123.
- [3] D.Y. Wu, S. Meure, D. Solomon, Self-healing polymeric materials: a review of recent developments, *Prog. Polym. Sci.* 33 (2008) 479–522.
- [4] H.N. Yow, A.F. Routh, Formation of liquid core polymer shell microcapsules, *Soft Matter* 2 (2006) 940.
- [5] D.Y. Zhu, M.Z. Rong, M.Q. Zhang, Self-healing polymeric materials based on microencapsulated healing agents: from design to preparation, *Prog. Polym. Sci.* 49–50 (2015) 175–220.
- [6] E.N. Brown, M.R. Kessler, N.R. Sottos, S.R. White, In situ poly(urea-formaldehyde) microencapsulation of dicyclopentadiene, *J. Microencapsul.* 20 (2003) 719–730.
- [7] M.W. Keller, N.R. Sottos, Mechanical properties of microcapsules used in a self-healing polymer, *Exp. Mech.* 46 (2006) 725–733.
- [8] B.J. Blaiszik, N.R. Sottos, S.R. White, Nanocapsules for self-healing materials, *Compos. Sci. Technol.* 68 (2008) 978–986.
- [9] X. Pan, D. York, J.A. Preece, Z. Zhang, Size and strength distributions of melamine-formaldehyde microcapsules prepared by membrane emulsification, *Powder Technol.* 227 (2012) 43–50.
- [10] B. Dong, Y. Wang, G. Fang, N. Han, F. Xing, Y. Lu, Smart releasing behavior of a chemical self-healing microcapsule in the stimulated concrete pore solution, *Cem. Concr. Compos.* 56 (2015) 46–50.
- [11] W. Xiong, J. Tang, G. Zhu, N. Han, E. Schlangen, B. Dong, et al., A novel capsule-based self-recovery system with a chloride ion trigger, *Sci. Rep.* 5 (2015) 10866.
- [12] G. Perez, E. Erkizia, J.J. Gaitero, I. Kaltzakorta, I. Jiménez, A. Guerrero, Synthesis and characterization of epoxy encapsulating silica microcapsules and amine functionalized silica nanoparticles for development of an innovative self-healing concrete, *Mater. Chem. Phys.* 165 (2015) 39–48.
- [13] J.-F. Su, Y.-Y. Wang, N.-X. Han, P. Yang, S. Han, Experimental investigation and mechanism analysis of novel multi-self-healing behaviors of bitumen using microcapsules containing rejuvenator, *Constr. Build. Mater.* 106 (2016) 317–329.
- [14] E.N. Brown, S.R. White, N.R. Sottos, Microcapsule induced toughening in a self-healing polymer composite, *J. Mater. Sci.* 39 (2004) 1703–1710.
- [15] R. Bagheri, R.A. Pearson, Role of particle cavitation in rubber-toughened epoxies: 1. Microvoid toughening, *Polymer (Guildf)* 37 (1996) 4529–4538.
- [16] H.S. Kim, M.A. Khamis, Fracture and impact behaviours of hollow microsphere/epoxy resin composites, *Compos. Part A: Appl. Sci. Manuf.* 32 (2001) 1311–1317.
- [17] M.A. El-Hadek, H.V. Tippur, Simulation of porosity by microballoon dispersion in epoxy and urethane: mechanical measurements and models, *J. Mater. Sci.* 37 (2002) 1649–1660.
- [18] Y.C. Yuan, M.Z. Rong, M.Q. Zhang, J. Chen, G.C. Yang, X.M. Li, Self-healing polymeric materials using epoxy/mercaptan as the healant, *Macromolecules* 41 (2008) 5197–5202.
- [19] M. Tripathi, D. Kumar, C. Rajagopal, Roy P. Kumar, Influence of microcapsule shell material on the mechanical behavior of epoxy composites for self-healing applications, *J. Appl. Polym. Sci.* 131 (2014) 40572.
- [20] E. Brown, N.R. Sottos, S.R. White, Fracture testing of a self-healing polymer composite, *Exp. Mech.* 42 (2002) 372–379.
- [21] E. Koh, N.-K. Kim, J. Shin, Y.-W. Kim, Polyurethane microcapsules for self-healing paint coatings, *RSC Adv.* 4 (2014) 16214.
- [22] J.D. Rule, N.R. Sottos, S.R. White, Effect of microcapsule size on the performance of self-healing polymers, *Polymer (Guildf)* 48 (2007) 3520–3529.
- [23] J.L. Moll, H. Jin, C.L. Mangun, S.R. White, N.R. Sottos, Self-sealing of mechanical damage in a fully cured structural composite, *Compos. Sci. Technol.* 79 (2013) 15–20.
- [24] M.M.C. Dailey, A.W. Silvia, P.J. McIntire, G.O. Wilson, J.S. Moore, S.R. White, A self-healing biomaterial based on free-radical polymerization, *J. Biomed. Mater. Res. A* (2013) 1–9.
- [25] M.R. Kessler, S.R. White, Cure kinetics of the ring-opening metathesis polymerization of dicyclopentadiene, *J. Polym. Sci., Part A: Polym. Chem.* 40 (2002) 2373–2383.
- [26] J.D. Rule, E.N. Brown, N.R. Sottos, S.R. White, J.S. Moore, Wax-protected catalyst microspheres for efficient self-healing materials, *Adv. Mater.* 17 (2005) 205–208.
- [27] S.H. Cho, H.M. Andersson, S.R. White, N.R. Sottos, P.V. Braun, Polydimethylsiloxane-based self-healing materials, *Adv. Mater.* 18 (2006) 997–1000.
- [28] M. Pelletier, A. Bose, Self-Mending Composites Incorporating Encapsulated Mending Agents, 2011. US20110316189 A1.
- [29] Z. Yang, J. Hollar, X. He, X. Shi, A self-healing cementitious composite using oil core/silica gel shell microcapsules, *Cem. Concr. Compos.* 33 (2011) 506–512.
- [30] J.F. Su, J. Qiu, E. Schlangen, Stability investigation of self-healing microcapsules containing rejuvenator for bitumen, *Polym. Degrad. Stab.* 98 (2013) 1205–1215.
- [31] M. Pelletier, R. Brown, A. Shukla, A. Bose, Self-Healing Concrete with a Microencapsulated Healing Agent, 2011. Kingston, USA.
- [32] J. Gilford III, M.M. Hassan, T. Rupnow, M. Barbato, A. Okeil, S. Asadi, Dicyclopentadiene and sodium silicate microencapsulation for self-healing of concrete, *J. Mater. Civ. Eng.* 26 (2014) 886–896.
- [33] E. Mostavi, S. Asadi, M.M. Hassan, M. Alansari, Evaluation of self-healing mechanisms in concrete with double-walled sodium silicate microcapsules, *J. Mater. Civ. Eng.* (2015). 04015035.

- [34] X. Wang, F. Xing, M. Zhang, N. Han, Z. Qian, Experimental study on cementitious composites embedded with organic microcapsules, *Materials (Basel)* 6 (2013) 4064–4081.
- [35] J.Y. Wang, H. Soens, W. Verstraete, N. De Belie, Self-healing concrete by use of microencapsulated bacterial spores, *Cem. Concr. Res.* 56 (2014) 139–152.
- [36] A. Kanellopoulos, T.S. Qureshi, A. Al-Tabbaa, Glass encapsulated minerals for self-healing in cement based composites, *Constr. Build. Mater.* 98 (2015) 780–791.
- [37] British Standards Institution, BS 1881-121:1983 Method for Determination of Static Modulus of Elasticity in Compression, 1983.
- [38] RILEM, Draft recommendation for in situ concrete strength determination by combined non-destructive methods., *Mater. Struct.* 26 (1993) 43–49.
- [39] C. Hall, T.K.-M. Tse, Water movement in porous building materials—VII. The sorptivity of mortars, *Build. Environ.* 21 (1986) 113–118.
- [40] M. Mooney, The viscosity of a concentrated suspension of spherical particles, *J. Colloid Sci.* 6 (1951) 162–170.
- [41] N. Frankel, A. Acrivos, On the viscosity of a concentrated suspension of solid spheres, *Chem. Eng. Sci.* 22 (1967) 847–853.
- [42] K. Toda, H. Furuse, Extension of Einstein's viscosity equation to that for concentrated dispersions of solutes and particles, *J. Biosci. Bioeng.* 102 (2006) 524–528.
- [43] J. Chong, E.B. Christiansen, A.D. Baer, Rheology of concentrated suspensions, *J. Appl. Polym. Sci.* 15 (1971) 2007–2021.
- [44] S.A. Faroughi, C. Huber, Crowding-based rheological model for suspensions of rigid bimodal-sized particles with interfering size ratios, *Phys. Rev. E* 90 (2014) 052303.
- [45] A. Ghanbari, B.L. Karihaloo, Prediction of the plastic viscosity of self-compacting steel fibre reinforced concrete, *Cem. Concr. Res.* 39 (2009) 1209–1216.
- [46] P. Giannaros, A. Kanellopoulos, A. Al-Tabbaa, Sealing of cracks in cement using microencapsulated sodium silicate, *Smar* (2016). Paper acce.
- [47] A.G. Evans, The strength of brittle materials containing second phase dispersions, *Philos. Mag.* 26 (1972) 1327–1344.
- [48] J. Lee, Fracture of glass bead/epoxy composites: on micro-mechanical deformations, *Polymer (Guildf)* 41 (2000) 8363–8373.
- [49] T. Kawaguchi, R.A. Pearson, The effect of particle-matrix adhesion on the mechanical behavior of glass filled epoxies: Part 1. A study on yield behavior and cohesive strength, *Polymer (Guildf)* 44 (2003) 4229–4238.
- [50] M.A. Wilson, W.D. Hoff, C. Hall, Water movement in porous building materials—XIII. Absorption into a two-layer composite, *Build. Environ.* 30 (1995) 221–227.